

Collisional transfer rates between excited levels in helium*

C. F. Burrell[†] and H.-J. Kunze[‡]*Department of Physics and Astronomy, University of Maryland, College Park, Maryland 20742*

(Received 20 July 1977; revised manuscript received 15 February 1978)

In an electron-beam plasma selective excitation by pulsed-dye-laser pumping has been used to study excitation transfer by electronic collisions. In particular, rate coefficients for the transitions $4^1P \rightarrow 4^1S$ and $3^1P \rightarrow 3^1S$ have been derived as well as the total deexcitation rate coefficient by $\Delta n \neq 0$ collisions of the 4^1P and 4^3D levels. The agreement with theoretical values is within the experimental uncertainties. The effective excitation transfer between the $n = 4$ singlet and triplet levels is higher than expected by about two orders of magnitude.

I. INTRODUCTION

Collisional transfer processes between excited states of atoms and ions not only influence or even dominate the relative populations of the various excited states, but also, as recognized some decades ago, affect most measurements of collisional cross sections for excitation from the ground state. Since it is impossible to measure the cross sections for these transitions between excited states directly in cross-beam experiments, one has attempted to infer the cross sections indirectly through careful analysis of emission lines either in beam experiments¹ or gaseous discharges.² More direct information was obtained through measurements of the relaxation mechanisms of specific excited states by selectively modulating the population through absorption of radiation.³ The great advances in pulsed-dye-laser technology opened new possibilities in this direction, and since the first demonstrations of the new possibilities in cold helium plasmas,^{4,5} more recent investigations in helium^{6,7} and hydrogen⁸ have been performed: in principle, the laser radiation is tuned to a suitable transition, and after enhancing the population of the upper level through absorption of a short laser pulse, the effective lifetime of this level is deduced from the exponential decay of proper emission lines. Although one obtains only the sum of all collisional and radiative loss rates from this level, specific rates can be deduced by changing the discharge parameters. A modification of these methods by using long-duration laser pulses allows measurements of lower state decay rates.⁹ In the following we describe measurements of $\Delta n = 0$ collisional transitions in a helium plasma generated by an electron beam.

II. DESCRIPTION OF THE EXPERIMENT

A. Experimental setup

The arrangement of the experiment is shown in Fig. 1. The electron beam was injected into a

vacuum chamber along its axis. This chamber consisted of a Pyrex tube 10 cm in diameter, around which two 150-turn coils were mounted in order to increase the efficiency of the electron gun and to confine the plasma radially; these coils maintained a magnetic field of 350 G at the center of the tube collinear with the electron beam.

The vacuum system was divided into two sections by a brass plate, to which the anode of the electron gun was affixed. The system was evacuated by a turbo-molecular pump on the cathode side of the brass plate while the helium gas was introduced on the opposite side. Under normal operating conditions there was a pressure ratio of 40:1 between the two sections. The experimental section of the system had a base pressure of typically 3×10^{-6} Torr.

The electron gun was of planar geometry and had a spacing of 4 mm between the cathode and the tungsten grid of the anode. The 1-cm diam., indirectly heated cathode, impregnated with BaO, yielded a continuous current of 0–40 mA at an applied anode voltage in the range of 0–300 V.

Four ports located between the two coils and at right angles to each other and to the axis permitted spectroscopic observations of the plasma and the introduction of the laser beam. The tunable dye laser, transversely pumped with the frequency-doubled beam of a Q-switched ruby laser, used a beam expander and an echelle grating to obtain a spectral resolution of 1 Å. The

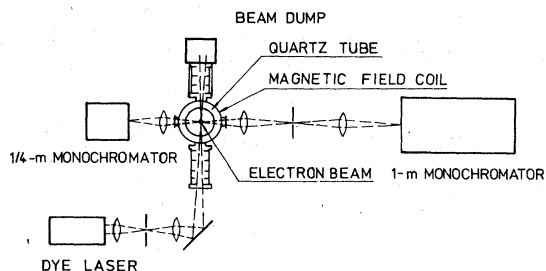


FIG. 1. Experimental setup.

laser output was focused through a 1-mm diam. aperture to reduce stray light, and then refocused into a 3-mm diam. spot at the center of the beam plasma. Light baffles at the entrance and the exit port of the laser beam reduced stray light further.

In a direction at right angles to the electron beam and the laser, the plasma radiation and the fluorescent emission of the optically pumped line were observed using a 1-m and a 0.25-m monochromator, respectively. The plasma radiation was detected after the monochromator by either an RCA 4459 or RCA C 31034A photomultiplier and displayed on a Tektronix 551 oscilloscope. Where sufficient light permitted, the time history of the enhanced emission was observed with fast time resolution by an Amperex model XP 1020 photomultiplier and displayed on a fast Tektronix model 519 oscilloscope. A shutter placed at an aperture stop of the optical system protected the photodetector from prolonged exposure to the radiation from the continuously operated plasma.

B. Determination of the plasma parameters

The electron temperature and density of the plasma were measured with an electric probe made of tungsten. The electron temperature was determined in the usual way from the slope of the semi-log plot of the electron current in the transition region of the probe characteristic.¹⁰ After subtracting the extrapolated ion current, the probe current-voltage relation agreed closely with an exponential fit over the range of one decade in probe current. We have used the numerical results of LaFramboise¹¹ to deduce the ion density from the ion saturation current.

A complication in the density measurement was the contribution to the probe current of the high-velocity electrons in the electron beam which were absorbed by the probe. We could estimate this effect and correct for it by measuring the probe current under condition of high vacuum when the probe current is caused only by electrons in the beam. While this is an approximation since the beam cross section will spread somewhat at higher fill pressures, we find that at fill pressures of 27 and 50 mTorr this effect is less than 30% of the ion saturation current.

C. Experimental technique

The rate of change of the population densities of any atomic system in a plasma is governed, in general, by a coupled set of rate equations taking into account all radiative and collisional processes to and from all other levels and the continuum. In a completely steady state these densities have relaxed towards equilibrium values. If this kinetic equilibrium is perturbed by intense pulsed radia-

tion the time-dependent densities can be calculated by solving the rate equations numerically, if all rate coefficients are known. On the other hand, a comparison between calculated population densities and measured ones allows a determination of rate coefficients if these are varied until observed and calculated population densities match.

The major difficulty inherent to this method, however, is to *isolate* the effect of one specific collision process from others: results of reasonable accuracy can be expected only if this collision process dominates the rates of all other collision processes to and from one specific level, and if the computed population density of this level, therefore, is most sensitive to the respective rate coefficient used in the theoretical computation. In addition, the perturbation created by the laser pulse should be large compared to the steady-state population especially if transitions between excited states are investigated, which are tightly coupled by these collisions. This can be achieved if the lower level of the optical pumping transition is a metastable state which is strongly overpopulated compared with most other excited states, and if lasers of sufficiently high intensity are used. The enhancement of the population density of the pumped level achieved in our experiments was so large, that the steady-state signal could be neglected completely.

Of the $\Delta n = 0$ collisions (rate coefficients X_0 with subscript 0) the transitions between the nS and nP states are the most promising ones with respect to the first condition: the S level couples only with the P level through a dipole transition, whereas the P level, in addition, also couples strongly with the D level. Furthermore, the theoretical cross section for the sum of all $\Delta n \neq 0$ collisions is smallest for the S level. For these reasons, we restricted our investigations to pumping the 4^1P , 3^1P , and 4^3D levels in helium.

Results of theoretical calculations of collisional transition rates as obtained in connection with the impact broadening of helium lines in plasmas¹² as well as the magnitude of steady-state population densities calculated by Drawin,¹³ for example, using a collisional-radiative model, permit the estimation of the various contributions to the total populating and depopulating rates of each specific level. In this way the whole set of rate equations can be simplified. Therefore in the computations we took into account for each level both radiative decay and collisional transfer into the levels of the same principal quantum number in the singlet or triplet system (rate coefficient X_0), and the total rate of deexciting collisions for $\Delta n \neq 0$ transitions from that level. This rate coefficient $X_T = \langle \sigma_T v \rangle$ was derived from a cross section calcu-

lated by Griem¹² in connection with the impact broadening of radio-frequency $n-\alpha$ lines.

$$\sum_{n',l',m'} \sigma_{nl} = \frac{4\pi a_0^2 n^2}{3Z^2} \left(\frac{1}{2}n^2 + \frac{3}{2}l^2 + \frac{3}{2}l + \frac{1}{2} \right) \times (E_H/E) \left[\frac{1}{2} + \ln(nE/ZE_H) \right] = \sigma_T \quad (1)$$

(the symbols have the usual meaning: n , l , and m are principal, orbital, and magnetic quantum numbers, E is the energy of the colliding electron, E_H is the Rydberg energy, a_0 is the Bohr radius, and Z is the effective charge on the outer electron).

The reverse $\Delta n \neq 0$ transfer rates from all levels into this same level were not included, since more detailed computations¹⁴ including levels up to $n = 10$ revealed no essential improvement of the results. The above model seemed justified specifically for the investigation of the $n^1S \rightarrow n^1P$ collisional transfer since the total rate coefficient $X_T(n^1S)$ for all $\Delta n \neq 0$ collisions from a n^1S level is expected to be much smaller than the rate coefficient $X_0(n^1S \rightarrow n^1P)$. The result, therefore, is not significantly perturbed by small changes in $X_T(n^1S)$.

To solve the rate equations two boundary conditions were used: either a time history for the pumping radiation was employed as given by the pulse shape of the incident laser beam, or the time history of the enhanced population density of the optically pumped level was used, which is reflected directly in the fluorescent emission from that level. The initial population densities were taken from Drawin,¹³ but their choice is not critical for our purposes. The population difference between upper and lower level of the pumping transition determines the absolute enhancement above the steady-state population of the upper levels which is achievable, whereas the time histories of the perturbations are practically independent of this choice, if kinetic equilibrium between the upper levels was established prior to the perturbation. Since for weak line intensities an oscilloscope with a longer rise time became necessary, the computer model also included the instrument response function $i(t-\tau)$: it was measured by driving the oscilloscope with a 0.5-nsec pulse from a Tektronix type 109 pulse generator. The response $f_2(t)$ to an arbitrary excitation $f_1(t)$ was determined by numerical integration of the convolution integral

$$f_2(t) = \int_0^t f_1(t') i(t-t') dt' \quad (2)$$

In practice, finally, we deduced the rate coefficients for collisions between excited states by investigating the changes induced in the level popu-

lations by the laser pulse in three different ways:

(i) The rate coefficients for excitation transfer between the singlet S and P level (for $n=3$ and 4) were determined by comparing experimental and calculated pulse shapes for the enhanced line emission.

(ii) If it becomes difficult to measure the pulse shapes of relatively weak signals or those of very rapid decay with sufficient accuracy, the time-integrated perturbations of the population densities could be utilized, too: their ratios were also determined by the respective rate coefficients, and values calculated with our model were used for comparison with experimental results. This way rate coefficients for the same transitions as mentioned above were measured again as well as an effective rate for singlet to triplet excitation transfer.

(iii) The decay rate of the optically pumped line was measured and compared with the predicted decay rate based on the deexcitation rate coefficients for $\Delta n \neq 0$ collisions.

III. EXPERIMENTAL RESULTS

A. Operation of the dye laser

The 4^1P , 3^1P , and 4^3D levels in helium were pumped by tuning the dye laser to the 3965-, 5015-, and 4471-Å He I spectral lines. Lasing at 3695 Å was achieved in a $3 \times 10^{-3}M$ solution of α NPO in ethanol; a 2 to 1 mixture (by volume) of ethanol solution of $2 \times 10^{-3}M$ acriflavine hydrochloride and $2 \times 10^{-3}M$ solution of 7-diethylamino-4-methylcoumarin in ethanol was used at the two other wavelengths.

The incident laser radiation was polarized 80% in the vertical plane, i.e., perpendicular to the B field. The polarization of the light emitted by the optically pumped levels was also measured, and the results are given in Table I. The polarization was independent of the electron density within the experimental accuracy and showed relatively slight dependence on the neutral density.

B. Plasma parameters

Figure 2 shows the electron temperature and the ratio of electron density to beam current as obtained with the electric probe for three filling pressures plotted as function of the anode voltage.

C. Rate coefficients

We consider first pumping of the 4^1P level and investigate the transfer to the 4^1S level through the analysis of the enhanced emission on the $4^1S - 2^1P$ transition at 5048 Å. Experimental and theoretical pulse shapes as obtained from the computer model were compared for various transfer

TABLE I. Polarization of the light emitted by the optically pumped level for three cases investigated.

Spectral line	Direction of polarization	Polarization P		
		$p = 10$ mTorr	27 mTorr	50 mTorr
3965 Å	Parallel to B	$36\% \pm 5\%$	$31\% \pm 5\%$	$28\% \pm 3\%$
5015 Å	Parallel to B		$6\% \pm 5\%$	$2\% \pm 3\%$
4471 Å	Orthogonal to B		$60\% \pm 7\%$	$61\% \pm 9\%$

rates as a function of electron density. For the comparison a pulse-shape factor $\tau = \tau(\frac{1}{2}) + \tau(\frac{1}{4}) + \tau(\frac{1}{8})$ was used instead of the decay rate [where $\tau(1/n)$ is the pulse duration between points where the intensity of the enhanced line emission is $1/n$ times the peak intensity], because it averages over a greater portion of the pulse shape and therefore should be less sensitive to random fluctuations.

Figure 3 shows the experimental pulse-shape factors as a function of electron density in comparison with theoretical values for two different excitation transfer rates at a fill pressure of 27 mTorr. The best fit obtained by the method of least squares is with a theoretical curve corres-

ponding to a rate coefficient $X_0(4^1P \rightarrow 4^1S) = 2.4 \times 10^{-5} \text{ cm}^3/\text{sec}$.

The corresponding results for the ratio of the integrated population enhancements of the 4^1S and 4^1P levels are plotted in Fig. 4. For unpolarized light this ratio may be simply deduced from the ratio of the measured line intensities; however, the proper relationship is somewhat more complicated, if the population of the 4^1P level is polarized. For the $4^1P \rightarrow 2^1S$ line the degree of linear polarization P parallel to the magnetic field for light propagating perpendicular to the field is defined as $P = (I_\pi - I_\sigma)/(I_\pi + I_\sigma)$, where I_π and I_σ are the components of the light intensity parallel and perpendicular to the field. P is related to the Zeeman sublevel population, and after some manipulation one finds for the ratio

$$\frac{N^*(S)}{N^*(P)} = \frac{A_p \lambda_s S(\lambda_p)}{A_s \lambda_p S(\lambda_s)} \frac{3}{3-P}, \quad (3)$$

where A is the transition probability, λ the wavelength, and S the corresponding sensitivity of the detector system. (This equation assumes equal

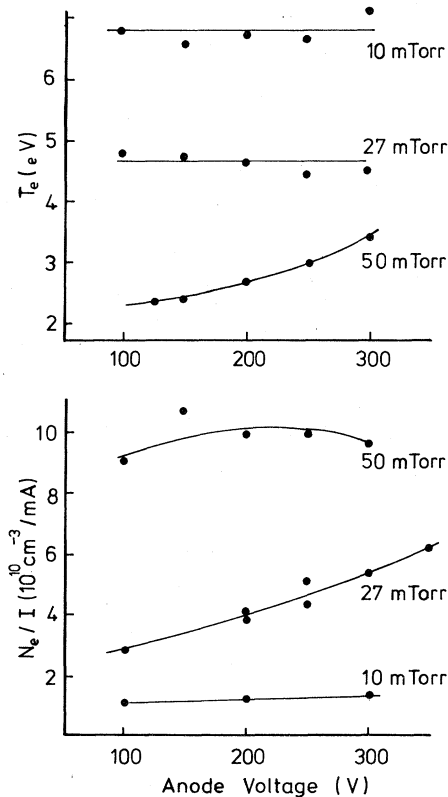


FIG. 2. Electron temperature and ratio of electron density to beam current as function of anode voltage for three filling pressures.

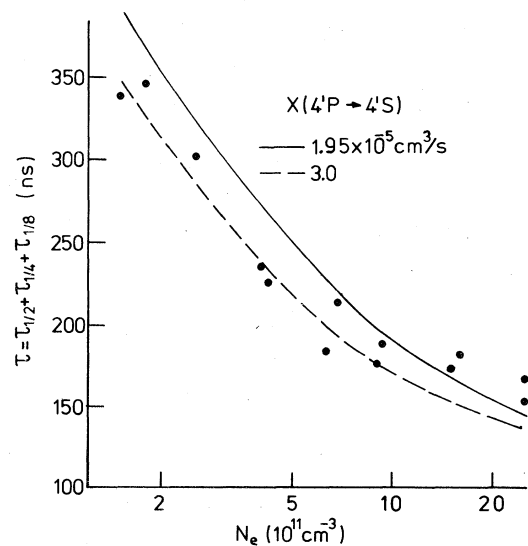


FIG. 3. Experimental pulse-shape factor τ . Calculated curves are shown for two different rate coefficients $X(4^1P \rightarrow 4^1S)$.

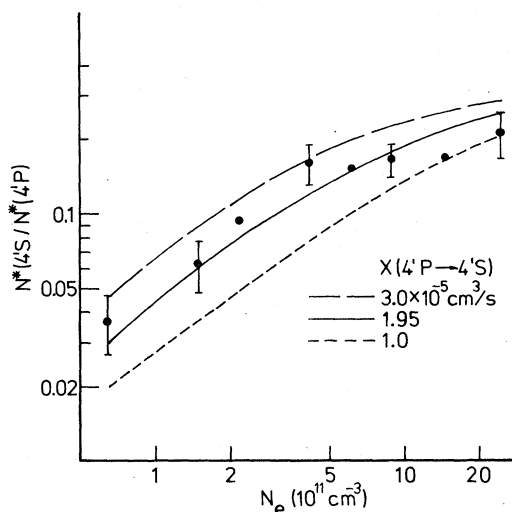


FIG. 4. Ratio of peak enhanced population densities of levels 4^1S and 4^1P as function of electron density. Calculated curves are shown for three different rate coefficients $X(4^1P \rightarrow 4^1S)$.

sensitivities of the detector system for the two components I_π and I_σ of the transition from the 4^1P level; if this is not the case, proper extension of the equation above becomes necessary.)

The optimum rate coefficient from this analysis again by the method of least squares is $X_0 = 2.0 \times 10^{-5} \text{ cm}^3/\text{sec}$, and combining the two results yields

$$X_0(4^1P \rightarrow 4^1S) = (2.2 \pm 0.7) \times 10^{-5} \text{ cm}^3/\text{sec}$$

at $T_e = 4.7 \text{ eV}$. The error quoted corresponds approximately to a 68% confidence interval for the standard deviation. The equivalent measurements for the $3^1P \rightarrow 3^1S$ collisional coupling were

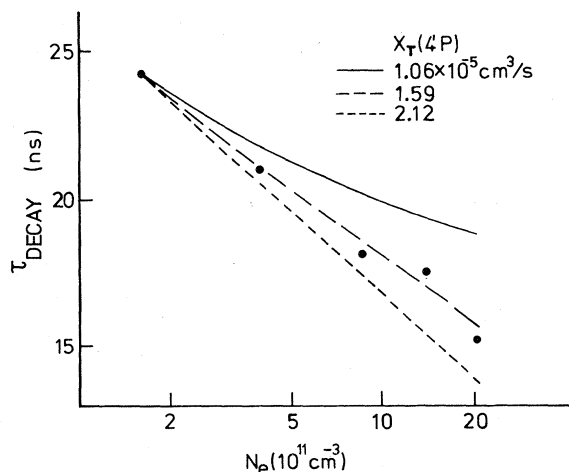


FIG. 5. Experimental decay time constant of the 4^1P level as function of electron density. Calculated curves are shown for three different values of the $\Delta n \neq 0$ collisional rate coefficient.

done at a neutral gas pressure of 50 mTorr in order to obtain the highest electron densities for sufficient excitation transfer.

The average result of both methods is

$$X_0(3^1P \rightarrow 3^1S) = (0.36 + 0.11) \times 10^{-5} \text{ cm}^3/\text{sec}$$

at $T_e = 2.8 \text{ eV}$.

The decay rate of the optically pumped level is a function of the total rate of deexciting collisions and the total radiative lifetime. The decay time constant was measured between $\frac{1}{2}$ and $\frac{1}{8}$ of the peak intensity. Figure 5 shows the experimental results for the 4^1P level and theoretical curves obtained with the computer model for different values of the rate coefficient X_T for $\Delta n \neq 0$ collisions. In the model, all rate coefficients for $\Delta n = 0$ collisions were calculated with the high-temperature limit rate coefficient of Griem *et al.*¹⁵:

$$X_0(l \rightarrow l-1) = 3 \left(\frac{2\pi m}{kT} \right)^{1/2} \left(\frac{\hbar}{m} \right)^2 \frac{1}{Z^2} \times \frac{n^2 l(n^2 - l^2)}{2l + 1} \ln \left(\frac{2ZkT}{n^2 \Delta E} \right). \quad (4)$$

The rate coefficients $X_0(l \rightarrow l-1)$ were derived from $X_0(l \rightarrow l-1)$ using the principle of detailed balance. The decay rate observed in the singlet system is much more rapid than would be expected if the resonance lines were completely trapped. The absorption coefficients at the line center for the resonance lines $4^1P \rightarrow 1^1S$ and $3^1P \rightarrow 1^1S$ are 16.3 and 40.9 cm^{-1} at neutral-helium pressure of 27 mTorr and at room temperature. However, a resonance line photon will contribute to the observable decay of the n^1P level if it escapes the region of the plasma viewed by the monochromator. The geometry is difficult and an analytic solution is unobtainable, but we can evaluate the importance of this decay mode by estimating that the photon must travel approximately 2 mm to escape. From the calculations of Phelps,¹⁶ the escape factor g is found to be 0.2 and 0.05 for the two transitions, resulting in effective radiative decay rates

$$A_{\text{eff}} = gA \text{ of } A_{\text{eff}}(4^1P \rightarrow 1^1S) = 4 \times 10^7 \text{ sec}^{-1}$$

and

$$A_{\text{eff}}(3^1P \rightarrow 1^1S) = 3 \times 10^7 \text{ sec}^{-1},$$

respectively; these are larger than the corresponding radiative transition rates for $n^1P \rightarrow 2^1S$ transitions.

Therefore, we included the radiative transition rate $A_{\text{eff}} = gA(n^1P \rightarrow 1^1S)$ in the computations with an empirical escape factor adjusted so that experimental and computed decay time constants agreed at the lowest electron density—where the decay is least sensitive to the collision processes.

The best agreement between the theoretical curves and the experimental data is obtained for the $\Delta n \neq 0$ rate coefficients

$$X_T(4^1P) = (1.7 \pm 0.3) \times 10^{-5} \text{ cm}^3/\text{sec}$$

at $T_e = 4.7$ eV,

$$X_T(4^3D) = (2.3 \pm 0.6) \times 10^{-5} \text{ cm}^3/\text{sec}$$

at $T_e = 4.7$ eV.

The decay rate of the 3^1P level was insensitive to rate coefficient X_T in comparison with experimental uncertainties. In this case, the dependence of the decay rate on the electron density is a function primarily of the $\Delta n = 0$, $\Delta l = \pm 1$ collisions, and the total experimental rate coefficient for deexcitation of the 3^1P level by collisions is found

$$\begin{aligned} X_{\text{tot}}(3^1P) &= X_T(3^1P) + X_0(3^1P \rightarrow 3^1S) + X_0(3^1P \rightarrow 3^1D) \\ &= (2.5 \pm 0.4) \times 10^{-5} \text{ cm}^3/\text{sec}. \end{aligned}$$

We also investigated the collisional transfer from singlet to triplet levels by pumping the 4^1P level and observing the $4^3D \rightarrow 4^3P$ transition at 4471 \AA . The ratio of the enhanced population densities $N^*(4^3D)/N^*(4^1P)$ as a function of the electron density is shown in Fig. 6. The result clearly indicates that electronic transitions are involved in the excitation transfer. If one interprets the observations as being due to direct collisional transfer between the two levels, one obtains an effective rate coefficient

$$X_{\text{eff}}(4^1P \rightarrow 4^3D) = 1.5 \times 10^{-5} \text{ cm}^3/\text{sec}$$

at $T_e = 4.7$ eV.

No transfer between singlet and triplet $n=3$ levels was detectable.

IV. DISCUSSION

Table II summarizes the experimental rate coefficients. They may be compared with theoretical

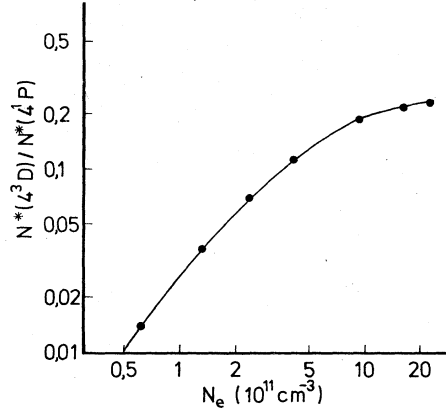


FIG. 6. Ratio of peak enhanced population densities of levels 4^3D and 4^1P as function of electron density for level 4^1P being pumped.

values according to Eqs. (1) and (4). The errors quoted correspond to about a 68% confidence interval for the standard deviation; they were derived, of course, under the assumption that not only the computer model describes correctly the time behavior of the population densities but also the other rate coefficients not varied for the best fit either do not influence the results or are known with sufficient accuracy. As discussed in Sec. IIC, extension of our model to include more levels does not significantly influence the specific results obtained here.

The total rate coefficient $X_{\text{tot}}(3^1P)$ for the sum of all $\Delta n \neq 0$ and $\Delta n = 0$ deexciting collisions of the 3^1P level is independent of other rate coefficients than those given by Eqs. (1) and (4), and the experimental value agrees with the theoretical result within the error limits. This shows that theory predicts at least the sum of these rates correctly. The dominant rate coefficient will be $X_0(3^1P \rightarrow 3^1D)$, while $X_T(3^1P)$ can be neglected.

TABLE II. Experimental rate coefficients.

T_e (eV)	Rate coefficients (cm^3/sec)
4.7	$X_0(4^1P \rightarrow 4^1S) = (2.2 \pm 0.7) \times 10^{-5}$
2.8	$X_0(3^1P \rightarrow 3^1S) = (0.36 \pm 0.11) \times 10^{-5}$
4.7	$X_T(4^1P) \approx 1.7 \times 10^{-5}$
4.7	$X_T(4^3D) \approx 2.3 \times 10^{-5}$
2.8	$X_{\text{tot}}(3^1P) = X_T(3^1P) + X_0(3^1P \rightarrow 3^1S) + X_0(3^1P \rightarrow 3^1D)$ $= (2.5 \pm 0.4) \times 10^{-5}$
4.65	$X_{\text{eff}}(4^1P \rightarrow 4^3D) = 1.5 \times 10^{-5}$

The rate coefficient $X_0(4^1P \rightarrow 4^1S)$ was derived from the time history of the population of the 4^1S level, and this result is influenced only by the theoretical choice of $X_T(4^1S)$ for the 4^1S level. The theoretical results predict a ratio $X_0(4^1S \rightarrow 4^1P):X_T(4^1S) \approx 10:1$ which indeed justifies our analysis: an underestimate of $X_T(4^1S)$ by a factor of 12 which is considered unlikely, would decrease our experimental value of $X_0(4^1P \rightarrow 4^1S)$ by a factor of 2. Both experimental values for $X_0(4^1P \rightarrow 4^1S)$ and $X_0(3^1P \rightarrow 3^1S)$ agree with the theoretical rate coefficient of Griem to within 10% and 20%, respectively. A large discrepancy is observed with the only other experimental value reported by Wellenstein and Robertson.³ In a glow discharge these authors obtain a cross section $\sigma(3^1P \rightarrow 3^1S) = (2.8 \pm 0.8) \times 10^{-16} \text{ cm}^2$. At an average temperature of $T_e = 5 \text{ eV}$ in their discharge, this corresponds to a rate coefficient $X_0(3^1P \rightarrow 3^1S) \approx 3.5 \times 10^{-8} \text{ cm}^3/\text{sec}$, which is smaller than the value we have measured by about two orders of magnitude.

The total rate coefficients X_T for the $\Delta n \neq 0$ deexciting collisions were derived under the assumption the rate coefficients X_0 being given by Eq. (4), which we believe now justified according to the results discussed above. A comparison of $X_T(4^1P)$ with $X_0(4^1P \rightarrow 4^1S)$ and $X_0(4^1P \rightarrow 4^1D)$ suggests, however, that this measurement might be subject to large inherent uncertainties, the $\Delta n = 0$ collision rates being the larger ones. Therefore, we varied the theoretical $\Delta n = 0$ collision rates in the analysis of the experimental data by 20%: we observed a change of the experimental result for X_T by 10% only. This can be explained because the $\Delta n = 0$ transitions rapidly saturate.

The values derived are 1.7 and 1.5 times larger than the theoretical results according to Eq. (1), which should not be surprising either, since they include also the effect of intersystem ($\Delta S \neq 0$) collisions.

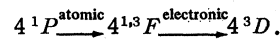
If we do the comparison with the rate coefficients X_T calculated according to the effective Gaunt factor approximation of Seaton¹⁷ and Van Regemorter¹⁸ (which is valid, of course, only for $\Delta l = \pm 1$ transitions), we obtain a similar result with the experimental values being here 1.2 and 1.5 times larger.

The strong excitation transfer between the 4^1P and 4^3D levels is unexpected. If it is due to a direct electronic collision it requires a cross section which is several orders of magnitude greater than theoretical estimates.¹⁹

On the other hand, the spin is not a good quantum number for the $4F$ states in helium²⁰; the mixing coefficient between the levels 4^1F and 4^3F being about 0.6.²¹ Therefore, one could propose that

at first the excitation be transferred from the 4^1P level to the 4^3D level by multiple electronic collisions. In the limit of low electron density, however, the enhancement of the 4^3D level should then be proportional to N_e^q where q is the number of electronic collisions in the process. We observe $q = 1$ in the limit of low electron density.

A combination of a single electronic collision and an atom-atom collision could explain the results. Several researchers^{22,23} have reported a large atomic cross section for the $\Delta L = 2$ transition $4^1P \rightarrow 4^{1,3}F$: they find $\sigma \approx 2 \times 10^{-14} \text{ cm}^2$. This will cause excitation transfer between the 4^1P and 4^3D levels by the two-step process



This atomic cross section was included in a collisional radiative model,²⁴ which contained all singlet-singlet and triplet-triplet electronic collisions up to $n = 6$. To explain our experimental results by this process an atomic cross section an order of magnitude greater than reported would be required.

If we compare our experimental curves in detail (for example, see Figs. 3 and 4), we recognize a systematic divergence of the experimental points from the theoretical curves at high electron densities corresponding to smaller rate coefficients $X_0(n^1P \rightarrow n^1S)$. One could think of several possible explanations for this behavior:

(a) Collision processes other than electron-atom collisions may be important. We have assumed to this point, that the energy gap between S and P levels (for $n = 3$ and 4) is large compared to the thermal energy of the neutrals. The ratio of energy gap to thermal energy is 2.5 and 6 for $n = 3$ and 4, respectively. If we take the experimental cross section $\sigma(3^1P \rightarrow 3^1S)$ of Wellenstein and Robertson³ for atom-atom collisions, we find that the collision rate is two orders of magnitude less than the radiative decay rate and represents less than 10% of the electronic collision rate at the lowest electron density; it is therefore not significant in view of the experimental uncertainties. The low velocity of the ions and relatively large energy gaps between levels also mean that the rate coefficient for inelastic ion collisions is negligible. Finally, the neglect of inelastic collisions caused by the high-energy electrons in the electron beam is justified, because the density ratio of plasma electrons to beam electrons is 10^3 , and the rate coefficient has a dependence on the electron energy of $\ln(E)/\sqrt{E}$.

(b) There might be a systematic error in the plasma density measurement such that the density is overestimated for high densities or underestimated at low density. Within a density regime

from 10^9 to 10^{11} cm^{-3} Keen and Fletcher²⁵ compared measurements of plasma density by the double probe method and by a resonant microwave cavity technique and found them to be in reasonably close agreement, so we would like to rule out systematic errors of the probe measurements, too.

ACKNOWLEDGMENTS

The authors would like to express their appreciation to H. R. Griem for many valuable discussions. This work was supported by the NSF.

*The material in this article contains part of a thesis submitted 1974 in partial fulfillment of the requirements for the Ph.D. degree at the University of Maryland.

†Present address: Lawrence Berkeley Laboratory, University of California, Berkeley, Calif. 94720.

‡Present address: Institut für Experimentalphysik, Ruhr-Universität, 463 Bochum, West Germany.

¹R. J. Anderson, R. H. Hughes, and T. G. Norton, *Phys. Rev.* **181**, 198 (1969).

²L. C. Johnson and E. Hinnov, *Phys. Rev.* **187**, 143 (1969).

³H. F. Wellenstein and W. W. Robertson, *J. Chem. Phys.* **56**, 1072 (1972).

⁴C. F. Burrell and H.-J. Kunze, *Phys. Rev. Lett.* **28**, 1 (1972).

⁵C. B. Collins, B. W. Johnson, and M. J. Shaw, *J. Chem. Phys.* **57**, 5310 (1972).

⁶J. P. Moy, J. C. Gauthier, J. P. Geindre, *Proceedings of the XIIIth International Conference, Phenomena in Ionized Gases, Eindhoven, 1975* (North-Holland, Amsterdam, 1975), p. 16.

⁷A. Catherinot, B. Dubreuil, A. Bouchoule, and P. Davy, *Phys. Lett. A* **56**, 469 (1976).

⁸K. Bergstedt, G. Himmel, and F. Pinnekamp, *Phys. Lett. A* **53**, 261 (1975).

⁹D. D. Burgess and C. H. Skinner, *J. Phys. B* **7**, L297 (1974).

¹⁰F. F. Chen, "Electric Probes," in *Plasma Diagnostic*

Techniques, edited by R. H. Huddleston and S. L. Leonard (Academic, New York, 1965).

¹¹J. G. LaFramboise, Univ. of Toronto, Inst. for Aerospace Studies, Report No. UTIAS-100 (1966).

¹²H. Griem, *Spectral Line Broadening by Plasmas* (Academic, New York, 1974), Eqs. (467) and (478).

¹³H. W. Drawin, *Z. Naturforsch. A* **19**, 1451 (1964).

¹⁴C. F. Burrell, Ph.D. thesis (University of Maryland, 1974), Department of Physics and Astronomy, Technical Report No. 74-094.

¹⁵Reference 12, p. 70.

¹⁶A. V. Phelps, *Phys. Rev.* **110**, 1362 (1958).

¹⁷M. J. Seaton, in *Atomic and Molecular Processes*, edited by D. R. Bates (Academic, New York, 1962), p. 374.

¹⁸H. Van Regemorter, *Astrophys. J.* **136**, 906 (1962).

¹⁹M. Blaha, Univ. of Maryland (private communication).

²⁰R. M. Paris and R. W. Mires, *Phys. Rev. A* **4**, 2145 (1971).

²¹R. K. van der Eynde, G. Wiebes, and Th. Niemyer, *Physica* **59**, 401 (1972).

²²R. B. Kay and R. H. Hughes, *Phys. Rev.* **154**, 154 (1967).

²³Dempsey E. Lott III, R. E. Glick, and J. A. Llewellyn, *J. Quant. Spectros. Radiat. Transfer* **15**, 513 (1975).

²⁴R. A. Hess and C. F. Burrell, *Bull. Am. Phys. Soc.* **20**, 1295 (1975).

²⁵B. E. Keen and W. H. W. Fletcher, *J. Phys. D* **4**, 1695 (1971).